ChemInform Abstract: Dissymmetries in Fluorescence Excitation and Emission from Single Chiral Molecules

ARTICLE *in* CHIRALITY · JANUARY 2009

Impact Factor: 1.89 · DOI: 10.1002/chir.20809 · Source: PubMed

7 AUTHORS, INCLUDING:

Ruthanne Hassey Paradise
University of Massachusetts Amherst
11 PUBLICATIONS **170** CITATIONS
SEE PROFILE

Austin Cyphersmith
University of Massachusetts Amherst
6 PUBLICATIONS **45** CITATIONS
SEE PROFILE

Dhandapani Venkataraman
University of Massachusetts Amherst
114 PUBLICATIONS **4,347** CITATIONS
SEE PROFILE

Michael D Barnes
University of Massachusetts Amherst
147 PUBLICATIONS **2,324** CITATIONS
SEE PROFILE

CHIRALITY 21:E265–E276 (2009)

Dissymmetries in Fluorescence Excitation and Emission from Single Chiral Molecules

RUTHANNE HASSEY-PARADISE, AUSTIN CYPHERSMITH, ANNA MAY TILLEY, TIM MORTSOLF, DIPANKUR BASAK, DHANDAPANI VENKATARAMAN, AND MICHAEL D. BARNES*

George R. Richason Research Laboratory, Department of Chemistry, University of Massachusetts-Amherst, Amherst, Massachusetts 01003.

Contribution to the Special Thematic Project "Advances in Chiroptical Methods"

ABSTRACT Chirality in molecular systems plays profoundly important roles in chemistry and physics. Most chemistry students are introduced to the concept of chirality through demonstrations of the interaction of chiral molecules with polarized light manifested as an "optical rotation" leading to the "(+)" and "(−)" [or dextrorotatory (*d*-) and levorotatory (*l*-)] designations of chiral compounds, with the subsequent determination of absolute stereochemical configuration by chemical or physical means enabling application of the familiar "*R*" and "*S*" labels. Although the *intrinsic* molecular parameters that control the dissymmetric light-matter interaction in chiral systems are well understood, we have only recently begun to ask questions regarding the role of local molecular environment and hidden heterogeneities associated with the ensemble-averaged molecular chiroptical response. In this mini-review, we discuss some of our recent research on application of single-molecule spectroscopy as a tool for probing heterogeneities and fluctuations of chiroptical dissymmetries in condensed phase. *Chirality 21:E265–E276, 2009.*

KEY WORDS: single-molecule; chiroptical spectroscopy; fluorescence excitation; circularly polarized luminescence

INTRODUCTION

For more than 200 years, scientists of virtually all disciplines—Optics, Physics, Chemistry, and Biology—have enjoyed an intense fascination with molecular chirality and the dissymmetric interaction of chiral systems with circularly polarized light.[1–7] In physics, dissymmetries are manifested at the most fundamental subatomic material level.[8–10] In biology and chemistry, molecular chirality plays a key role in biochemical synthesis,[11–15] molecular recognition,[16–30] and self-assembly[17,31–49] processes in nature. More recently, studies of supramolecular chiral assemblies in natural systems have inspired new directions in chiral photonics.[50] A great wealth of data on the dissymmetric chiroptical response on ensembles of structurally identical chiral systems has been obtained from spectroscopic tools such as optical rotatory dispersion (ORD)[51–55] and circular dichroism (CD),[2,56] fluorescence detected circular dichroism (FDCD).[29,57–71] Combined with detailed theoretical analysis, these tools lead ultimately to assignment of absolute chiral configurations from spectroscopic data.[72–82] However, an important aspect of this interaction that remains poorly understood—in particular for condensed phase systems—is the role of local molecular environment and configurational fluctuations that could result in a significant heterogeneity in the chiroptical response of isolated molecular systems.[83]

The idea of molecular chirality and its manifestation through a dissymmetric interaction with polarized light is introduced in chemistry courses at the introductory level. An object is said to be chiral if the object and its mirror image are not superimposable; that is, the object cannot be mapped onto its mirror image by any combination of rotations and translations.[1] For chiral molecular systems, this is manifested in a nonresonant light interaction through a different bulk polarizability (refractive index) for right- and left-circularly polarized radiation. In resonant molecular transitions for chiral materials, the origin of the dissymmetric response derives from a combination of the electric transition dipole, and the magnetic transition dipoles; thus, the product of electric and magnetic transition dipoles has a specific handedness, giving rise to absorption cross sections for light of right or left circular polarization. Both the sign and magnitude of this dissymmetric response—measured as either a differential absorbance or phase-retardance (polarization rotation angle) for resonant or nonresonant interactions, respectively—is captured in the dissymmetry parameter, "*g*."

Contract grant sponsor: US DOE Basic Energy Sciences; Contract grant number:DE-FG02-05ER15695.
Contract grant sponsor: NSF-Sponsored MRSEC.
Contract grant sponsor: National Science Foundation; Contract grant number: CHE-0848596.
*Correspondence to: Michael Barnes, George R. Richason Research Laboratory, Department of Chemistry, University of Massachusetts-Amherst, Amherst, MA 01003, USA. E-mail: mdbarnes@chem.umass.edu
Received for publication 30 June 2009; Accepted 28 September 2009
DOI: 10.1002/chir.20809
Published online 10 December 2009 in Wiley InterScience (www.interscience.wiley.com).

The theory of light-matter interactions with chiral materials has been very well established;[1] here, we summarize very briefly some points relevant to single-molecule chiroptical spectroscopy. For a transition between initial and final states $|\, i >$, and $|\, f >$, the *Rotatory Strength Tensor*, $\mathbf{R}_{f\leftarrow i}$, is defined as

$$\mathbf{R}_{f\leftarrow i} = -\left\{\frac{1}{3}\omega_{f\leftarrow i}\cdot Re(\vec{\mu}\times\vec{\vec{\Theta}}) - \mathrm{Im}(\vec{\mu}\bullet\vec{m})\right\}, \qquad (1)$$

where the quantities $\vec{\mu}$ and $\vec{m}$ represent the electric (E1), magnetic (M1) transition dipole moments, respectively (i.e., $\mu_x = <f|-e\cdot\hat{X}|i>$), and $\vec{\vec{\Theta}}$ is the electric quadrupole (E2) tensor. Equation 1 indicates that there are two contributions to the overall rotatory strength tensor: The (symmetric) tensor product $[\vec{\mu}\times\vec{\vec{\Theta}}]$, which describes electric dipole/electric quadrupole coupling, and the (antisymmetric) $[\vec{\mu}\bullet\vec{m}]$ scalar product that describes the electric dipole/magnetic dipole coupling. For observation along the *z*-axis, the rotatory strength can be expressed as

$$\mathbf{R}^{z}_{f\leftarrow i} = -\left\{\frac{1}{3}\omega_{f\leftarrow i}\cdot Re(\hat{z}\bullet[\vec{\mu}\times\vec{\vec{\Theta}}]\bullet\hat{z}) - \mathrm{Im}(\vec{\mu}_z\bullet\vec{m}_z)\right\}. \qquad (2)$$

In general, we can define a rotatory strength for any arbitrary observation direction along the unit vector $\hat{n}$ with orientation defined by polar angles θ and ϕ,[84]

$$\begin{aligned}\Gamma_{\hat{n}}(\theta,\phi) = \hat{n}\cdot\mathbf{R}_{f\leftarrow i}\cdot\hat{n} = \sin^2\theta[R_{xx}\cos^2\phi + R_{yy}\sin^2\phi \\ + \frac{1}{2}(R_{xy}+R_{yx})\sin(2\phi)] + \sin(2\theta)[\frac{1}{2}(R_{xz}+R_{zx})\cos\phi \\ + \frac{1}{2}(R_{yz}+R_{yx})\sin\phi] + \cos^2\theta\cdot R_{zz} \qquad (3)\end{aligned}$$

giving the dissymmetry parameter (for a specific orientation angle) as,

$$g_{\hat{n}} = \frac{4\Gamma_{\hat{n}}(\theta,\phi)}{cD(\hat{n})} \qquad (4)$$

where $D(\hat{n})$ is the dipole strength perpendicular to the observation angle.

$$D(\hat{n}) = (\vec{\mu}\cdot\vec{\mu} - (\hat{n}\cdot\vec{\mu})^2) \qquad (5)$$

For isotropic samples, contributions from quadrupole interactions vanish, giving a rotatory strength that appears a product of electric and magnetic dipole matrix elements, thus reducing to the familiar dissymmetry expression,

$$g = -\frac{2}{3c}\mathrm{Im}(\mu_x m_x + \mu_y m_y + \mu_z m_z) \qquad (6)$$

giving rise to a range of dissymmetry values of $-2 < g < +2$. [made sure all notation is consistent]

In solution or unoriented solid phases, approximating the rotatory strength (hence the dissymmetry parameter) in an isotropic limit is usually quite good since all orientations are sampled. For isolated molecules in crystals[56,85–88] or polymer-supported films—the typical experimental format used for single-molecule spectroscopy—the fixed (or strongly restricted) molecular orientation implies that both E1-M1 and E1-E2 interactions contribute to the measured dissymmetry. In FDCD, or Circularly Polarized Luminescence (CPL)[89–101] where an (ensemble) fluorescence signal is used as a reporter of total absorption, it was recognized early on that the isotropic limit fails when the rotational diffusion time of the molecule is long compared to the fluorescence lifetime, as is the case in viscous solvents.[68,70,71] In such a case, contributions from electric dipole/electric quadrupole interactions can strongly modify or distort the measured dissymmetry. It is interesting to point out that work from Kahr and coworkers have shown that achiral species (even water!) with a well-defined orientation may show a dissymmetric chiroptical response.[102]

In addition to orientation effects, molecular solvation and local environment are known to strongly modify the chiroptical response of an isolated molecule, yet remain poorly understood.[103–105] In the elegant cavity ring-down polarimetry (CRDP) experiments by Vaccaro and coworkers,[52,54,106–113] solvation effects were observed to strongly modify the gas-phase optical rotatory dispersion of small chiral molecules. These, and recent theoretical efforts by Kongsted,[114–121] Crawford,[103,122–128] Autsbach,[51,129–133] and others, have pointed to the importance of the solvation environment in perturbing the electronic structure of the molecule, thus strongly affecting the chiroptical response.

The role of extrinsic factors is also clearly evidenced in condensed-phase measurements of dissymmetry in CPL from fluorescent chiral molecules.[92,96] Venkataraman and Riehl investigated the CPL for the chiral heterohelicenes in bulk solution, and obtained dissymmetery parameters of magnitude $\approx$0.001. In some larger molecular systems such as oligo(*meta*-phenylene ethynylene)s, Moore and coworkers have measured considerably larger ensemble-averaged *g*-values of $\approx$0.2,[134,135] and recently Bunz and Neher have reported average *g*-values as large as 0.37 in polyethylene ethynylene systems with chiral side-chains.[136,137] With a similar system, Swager and coworkers have demonstrated circular polarized luminescence and circular dichroism from chiral polyphenylene vinylene systems.[138] In an interesting contrast, Tew and coworkers report that their oligo(*ortho*-phenylene ethynylene)s—shown by 2D-NMR to have a tertiary structure similar to Moore's meta isomers—showed a net chiroptical response of nearly zero.[139–142] At the present time, it is difficult to reason the differences in the magnitude of the chiroptical responses for these chemically and structurally similar systems. Thus, there is a need to understand the factors that contribute to the "inhomogeneous broadening" (i.e., differences in local molecular environment, orientational, and configurational fluctuations.) of the molecular chiroptical response.

Over the past 15 years, advances in instrumentation and experimental methodologies in single-molecule imaging

and spectroscopy have provided an astounding wealth of information on dynamical processes in condensed phases.[143–147] Using single-molecule imaging techniques, researchers are now able to explore, with unprecedented clarity, details of individual molecular behavior, structure, and the coupling with local environment. The advent of ultrahigh precision time-to-digital converters, photon-counting avalanche photodiodes, and enhanced-sensitivity/high- speed charge-coupled device (CCD) imaging detectors coupled with high-numerical aperture microscopy platforms now provide access to a number of single-molecule fluorescence observables such as fluorescence lifetime,[60,144,148–150] "blinking" behavior,[151–163] spectral and spatial diffusion,[143,158,164–192] and polarization anisotropy.[149,150,193–201] In recent years, important new methodologies in single-molecule imaging have emerged including sub-diffraction limit spatial imaging, integration of scanning probe microscopies with fluorescence probes, multi-photon imaging, fluorescence resonant energy transfer (FRET), and molecular orientation determination by defocused emission pattern measurements.[202–214] Over the past 3 years, work in our group has focused on application of single-molecule imaging techniques to chiral fluorophores to begin to address these questions. In this mini-review, we summarize various aspects of single- molecule chiroptical spectroscopy (SMCS) and some of the interesting manifestations of chiroptical behavior at the single-molecule level.

How Does Single Molecule Spectroscopy Work?

Single molecule spectroscopy (SMS) was first developed by Moerner and coworkers in the late 1980s to investigate the nature of inhomogenous broadening of absorption spectra of dopant fluorophores in cryogenic organic crystals.[215,216] Later adapted to room-temperature systems by Xie,[201] and others, using a variety of elegant near- and far-field optical approaches, SMS has been applied to a vast number of biochemical and material sciences applications. Conventional single-molecule fluorescence imaging works on the principle of detecting large numbers of (10^5–10^8) fluorescence photons from a single probe molecule; spectral discrimination of the fluorescence is readily achieved through the large (typically tens of nm) Stokes shift in emission relative to the excitation wavelength.[217] This is conveniently implemented on research-grade microscope platforms using high ($\geq$1.3) numerical aperture objectives for efficient photon collection, high-sensitivity CCD cameras (or avalanche photodiodes) for efficient photon detection, along with some means for immobilizing the probe molecules (vis. Polymer-supported thin films, or biotin-streptavidin linkage) on a transparent substrate.

Quantitative information on single-molecule behaviors can be obtained on time-scales as short as 10–100 μs. Assuming an excitation flux large enough to saturate the absorption, the photon production rate from a single molecule approaches that of the spontaneous emission rate ($\approx$100 MHz); assuming overall photon detection efficiencies of $\approx$50%, one can detect a few thousand fluorescence photons on a 100-μs time interval. With current time-tagged/time-resolved photon-counting techniques coupled with pulsed-excitation, fluorescence lifetimes can accurately be determined within that nominal 100-μs time interval.[218,219] Of course, the stream of fluorescence photons arriving at the detector from a single molecule is not continuous, but is frequently interrupted through access to an excited electronic state that cannot relax to the ground state by radiative decay. This phenomenon is seen in virtually all single-molecule (or quantum dot) systems, is referred to as fluorescence intermittency, or "blinking." The mechanism of this process and associated time-scales vary, but for organic systems, it is generally accepted that blinking originates from an excited singlet to triplet intersystem crossing. Radiative decay from the triplet state is nominally forbidden, thus the molecule may remain "dark" for extended periods of time (typically on the order of a few tens to hundreds of microseconds). In addition to short-time instabilities, irreversible photochemical bleaching ultimately limits the total number ($\approx 10^8$–10^{10})

The choice of a single-molecule probe for SMCS must therefore be based on multiple spectral and stability criteria. First and foremost, because of spectral sensitivity constraints of most commercially available detectors, the probe candidate must have robust and stable fluorescence in the visible range of the electromagnetic spectrum (650–350 nm). Ideally, molecular systems should show a minimum of blinking to avoid obscuration of information on short timescales. Additionally, the total integrated fluorescence signal that can be extracted from a single molecule is ultimately limited by the average number of excitation-emission cycles that the molecule undergoes before irreversible photobleaching. In the design of a single-molecule chiroptical probe, where we are particularly interested in discerning dissymmetries in fluorescence excitation or circularly polarized luminescence, photostability on both short and long timescales are critical to the success of the experiment.

In earlier work, one of us (Venkataraman) demonstrated the synthesis of a new class of heterohelicenes that could be easily functionalized to build stable helical structures for electronic or optical applications.[220] This new synthetic scheme has enabled new fluorescent chiral probes that can be used to probe a variety of single-molecule chiroptical phenomena. The molecular frame also has a number of locations where the helicene can be attached to various molecular scaffolds, surfaces, or nanoparticles. Figure 1 shows the structures of these molecules based on triarylamines, along with bulk thin-film circular dichroism spectra. We have characterized the absorption and emission spectra of these molecules in various solutions, as well as solid films. The absorption maxima (λ_{max}) of 1, 2, and 3 are 442, 446, and 460 nm, with extinction coefficients (ϵ) of 22.6 $\times$ 10^3, 17.7 $\times$ 10^3, and 14.4 $\times$ 10^3 cm^{-1} M^{-1}, respectively. When excited at these wavelengths, 1, 2, and 3 emit at 460, 468, and 486 nm. In addition, we are able to isolate the atropisomers of 1 and 2 and verify the diastereomeric purity by proton NMR. In previous work, Riehl and Venkataraman were able to show that these molecules show a weak circular polarization in fluorescence; careful polarization analysis from solution phase bulk measure-

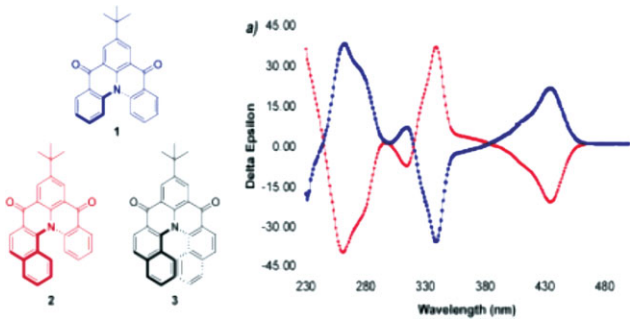

Fig. 1. (**A**) Chemical structures of (P1,P2, and P3) bridged triarylamine helicenes variants. In this study, the M2 and P2 diastereomers were used exclusively; (**B**) Thin-film circular dichroism spectra of the atropisomers of 1-camphanate (Blue = P1, RED = M1) of absorption-emission cycles that a molecule may undergo. [Color figure can be viewed in the online issue, which is available at www.interscience.wiley.com.]

ments of *P*1 and *M*1 enantiomers in solution (see Figure 3b) give (ensemble averaged) *g*-values of $+0.0009$ and -0.0011.[221]

Single-Molecule Studies of M2/P2 Heterohelicenes

As pointed out in the introductory section, the chiroptical signature of a single molecule is defined to a large extent by the chiral axis orientation with respect to the optical detection axis. In sample formats (e.g. solution phase) where the molecule samples all possible orientations on the timescale of the measurement, the off-diagonal elements of the Rotatory Strength tensor vanish, and the dissymmetry is defined by the familiar product of electric-dipole/magnetic dipole terms (eq. 6). For immobilized species required for single-molecule fluorescence imaging, orientational diffusion is either strongly hindered or completely nonexistent. In this case, off-diagonal elements of *R* (which may be orders of magnitude larger than the diagonal elements) define the orientation-dependent chiroptical dissymmetry. This can be seen by viewing R as a surface plot (see Figure 2) defined by the molecular-frame coordinates, where *Z* is the chiral axis of the molecule; the dissymmetry can appear either "positive" or "negative" depending on how the molecular frame is oriented with respect to the optic axis (and solid-angle of detection). In this simulation, the elements of R were determined using Time-dependent Density Functional theory at the B3LYP/6-31G(d) level of theory using a single optimized molecular geometry. Thus, it is highly desirable to have a priori (or independent) knowledge of the molecular orientation to make a meaningful comparison with theoretical calculation. Efforts aimed at determining the sensitivity of observation-angle dissymmetry with respect to level of theory and molecular conformational fluctuation is currently in progress.

Emission Pattern Imaging

Emission pattern imaging of single molecule fluorescence with a small (50–100 nm) defocusing has become a popular and well-established technique for probing transition dipole orientation in condensed phases.[209,213,214,222,223] The dipole emission pattern imaging technique readily recovers transition dipole moment orientation in the two polar angles θ, an ϕ by comparison with semiclassical electrodynamics simulation. The defocused radiation (antenna) patterns associated with single-molecule fluorescence are modeled using a point dipole electromagnetic source under a defocusing aberration, and the system interfaces (sample/microscope slide/immersion oil).[224,225] For a point dipole emitter, the emission intensity has a $\sin^2(\theta)$ distribution about the dipole axis, and this spatial anisotropy is mapped onto a distinct spatial pattern uniquely defined by the dipole orientation angles, θ and ϕ. To extract the orientation, one matches the experimentally obtained defocused single-molecule fluorescence image with a simulated image using the polar angles (and defocusing) as fitting parameters.[213]

The situation for chiral fluorophores is more complicated, but still tractable using a similar semiclassical approach. We have previously shown that defocused images from single helicene molecules are qualitatively different from those of single dipole emitters, manifested as a strong distortion in the radiation pattern that breaks the bilateral symmetry normally observed in emission patterns from linear dipole systems. Chiral chromophores have, in general, a transition moment possessing a finite electric quadrupole and magnetic dipole character. For a system with a *g*-value of order 0.1, this "effective" dipole (due to the quadrupole) can be a significant fraction (on the order of 1%) of the size of the "ordinary" transition electric dipole. It is therefore reasonable to anticipate a radiation pattern from a chiral source that would be qualitatively different from that of a pure linear dipole molecule.[226] We have carried out preliminary simulations of the defocused image obtained for the case of two coherently

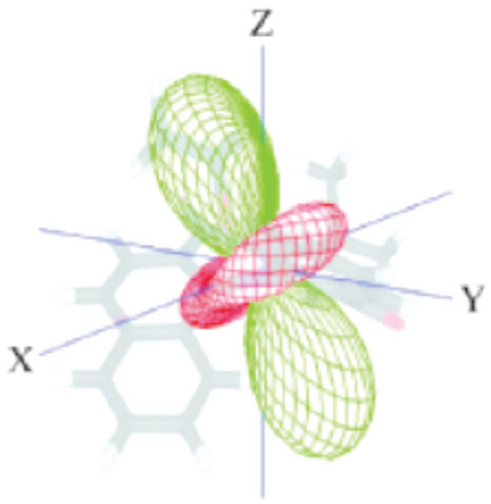

Fig. 2. Surface plot of $\Gamma(\theta,\phi)$ computed for M2 helicene superimposed on the molecular frame. The green and red color codings indicate positive and negative dissymmetries, respectively. Thus the angle-averaged dissymmetry (over the solid angle of the collection objective) is strongly orientation-dependent. [Color figure can be viewed in the online issue, which is available at www.interscience.wiley.com.]

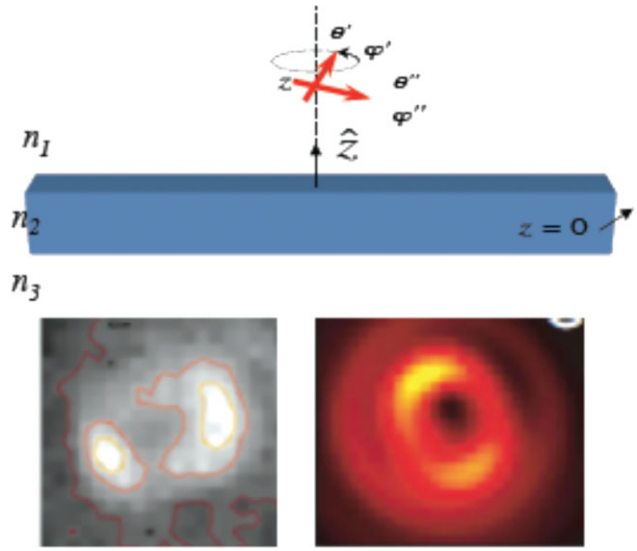

Fig. 3. Illustration of the semiclassical Kirkwood model used to simulate emission patterns from chiral fluorophores. Four different angles (referenced to surface normal) are used to specify the relative orientations of 2 coherently coupled dipoles. The resulting electromagnetic field is propagated through the dielectric interface to the detector plane. The lower left is an experimentally obtained defocused image from single helicene molecule, and lower right is a simulate image for the same defocusing (50 nm). [Color figure can be viewed in the online issue, which is available at www.interscience.wiley.com.]

added electric dipoles (Kirkwood model) having a relative phase shift. This is meant to roughly approximate the image pattern obtained from a long time integration of the radiation from a source with both an electric dipole and electric quadrupole character. More detailed calculations of these images for accurate electric quadrupole and magnetic dipole source characteristics are underway, and are expected from these considerations to yield defocused images that may be amenable to orientation analysis.

Dissymmetry in Fluorescence Excitation from Single Helicene Molecules

In a typical single-molecule fluorescence excitation experiment, the helicene concentration is adjusted to give ≈20 fluorescent spots in the illumination area (20 μm diameter). Linear-polarized laser excitation (457, 440, 405 nm) was passed through a broadband quarter waveplate to produce right- or left-circularly polarized light as desired. The purity in circular polarization, checked by retroreflection of the laser beam at the sample plane on the microscope, was determined to be >98° (the limit of our experimental accuracy). Once mounted on the microscope, the helicene-doped polymer films were illuminated with ≈100–200 μW of laser power, and the fluorescence was imaged with a high- sensitivity CCD camera (Roper Scientific PhotonMax). The single-molecule fluorescence count information was analyzed and background-subtracted using standard image-processing algorithms, and the fluorescence counts (after background subtraction) are recorded as a function of frame number (referred to as *intensity trajectories*) which can be correlated with a time, polarization or other externally controlled parameter. The helicene intensity trajectories show several of the hallmarks of single-molecule fluorescence including on-off blinking on sub-second timescales, and discrete photobleaching with a characteristic 1/e survival time (for ≈100 μW illumination power) of ≈20 sec.

A number of control experiments were performed to verify that the signals we measured did not arise from experimental artifacts. First, we looked the variation of fluorescence intensity as a function of right/left circular polarization from dye-doped polymer nanospheres. Figure 4 shows the histogram of apparent dissymmetry values obtained from ≈ 100 different nanospheres along with the distribution of dissymmetry parameters from P2 and M2 Helicene molecules excited with 457 nm radiation. The distribution of *g*-parameters for the nanospheres is symmetric about $g = 0$, characterized by a fullwidth- half maximum of ≈ 0.3. Similar measurements on single (achiral) linear dipole molecules (DiI_{18}) showed a distribution similar to the nanosphere sample (symmetric about $g = 0$), with a similar width.

For both sets of molecules, the integration time was set to 1 sec (long enough to average out much of the blinking), and 5 to 10 frames were acquired for a given laser polarization. Only molecules that survived at least 1.5 right/left excitation cycles were included in the analysis so that we could obtain (a) information on fluctuations of fluorescence intensity for a given excitation polarization, and (b) reproducibility of the mean fluorescence signals for different excitation polarizations. In virtually all the single-molecule intensity trajectories that we examined, the dissymmetry in fluorescence excitation appeared to be constant for the duration of the photochemical lifetime, although both positive and negative dissymmetry parameters were observed for a given diastereomer. The distributions of dissymmetry parameters obtained for M2 and P2

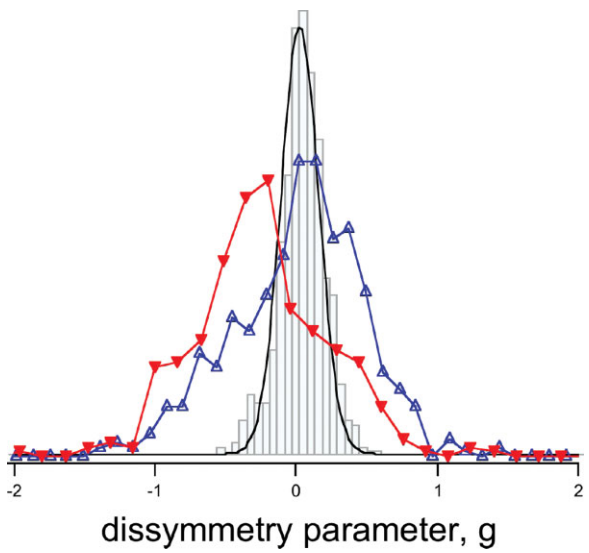

Fig. 4. Normalized probability distributions P(g) for dye-doped nanopsheres (black with gray histogram), P2 (blue), and M2 (red) diastereomers excited at 457 nm. [Color figure can be viewed in the online issue, which is available at www.interscience.wiley.com.]

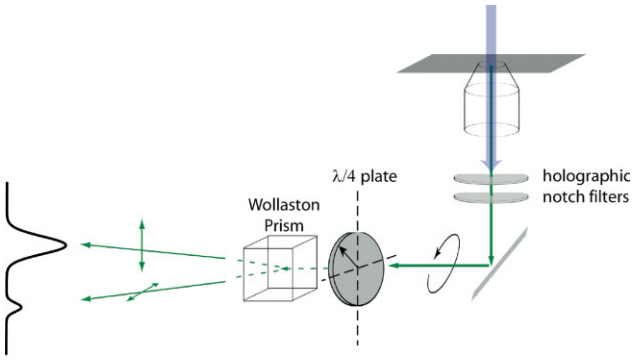

Fig. 5. Schematic of experimental configuration to probe dissymmetry in circular polarized luminescence (CPL) from single chiral fluorophores/nanostructures. The combination of fixed- orientation quarter waveplate and Wollaston prism enables relative intensities of right- and left-circularly polarized components of emission to be resolved on a single imaging camera. [Color figure can be viewed in the online issue, which is available at www.interscience.wiley.com.]

helicenes have been published previously. Briefly, these distributions (in particular with 457 nm excitation) are qualitatively different from those of the dye-doped nanosphere controls which are not symmetric about $g = 0$, and show a substantial width (~90% of the probability density contained within $g = \pm 1$. Recently, Cohen and coworkers have suggested that the breadth of our distribution was related to a linear polarization artifact introduced by the dichroic filter.[227] We emphasize that great care went into characterizing the polarization fidelity at the sample, and that a linear dichroism is not responsible for the signals we observe. We speculate that the major difference between Cohen's work and ours derives from the way in which the molecules are assayed. To follow single-molecule intensity trajectories over several 10s of seconds, the molecular subpopulation represented in our dissymmetry distributions necessarily reflects the highest photostability.

Dissymmetry in Fluorescence Emission from Single Helicene Molecules

In addition to fluorescence excitation measurements, we have recently initiated studies of the single- molecule chiroptical response in *emission*, or circularly polarized luminescence (CPL). In order to avoid any artifacts in CPL induced by *transmission* through the dichroic filter, we imaged the luminescence (and subsequent polarization analysis) without a dichroic filter. Figure 5 shows a schematic of the experimental configuration, where the sample was illuminated from above the microscope objective, directing the beam down through the collection objective, enabling a well-defined circular polarization in excitation to be used without a dichroic filter. Typically we used ≈100 μW of cw laser power; most of the excitation light is blocked from the detector using a high rejection ratio holographic notch filter (OD at notch wavelength >6), followed by a bandpass filter centered at 510 nm (FWHM 40 nm). To resolve the circularly polarized components in the fluorescence emsission, we used a λ/4 waveplate with fixed orientation coupled with a Wollaston prism. In this way, the single-molecule dissymmetry in emission can be determined on a frame-by-frame basis with a single multichannel detector with no moving parts in the detection optics.

Figure 6 shows some recently obtained data on dissymmetries in circular polarized emission from single (P2) helicenes using the experimental configuration described above. Single P2 molecules were isolated on a zeonex thin film, and excited with ≈100 μW of (*unpolarized*) 457-nm radiation. Imaging through the Wollaston prism resolves spatially the right (blue) and left (red) circularly polarized components of the emitted fluorescence. Each camera exposure thus constitutes a separate experiment in which we can determine the dissymmetry parameter on a frame-by-frame basis. The intensity trajectories for both RCP and LCP emission for three different P2 molcules is shown in Figure 6 along with the corresponding dissymmetry parameter trajectories. The error bars were established from characterization of the source noise of the sample. Interestingly, in these examples of P2 fluorescence using unpolarized excitation, we observed some single-molecule signals in which the dissymmetry parameter fluctuates between positive and negative values. In addition, we have shown that dissymmetry parameters of order unity can be seen with high signal to noise ratio in fluorescence emission. We are currently exploring the excitation polarization dependence of emission dissymmetries.

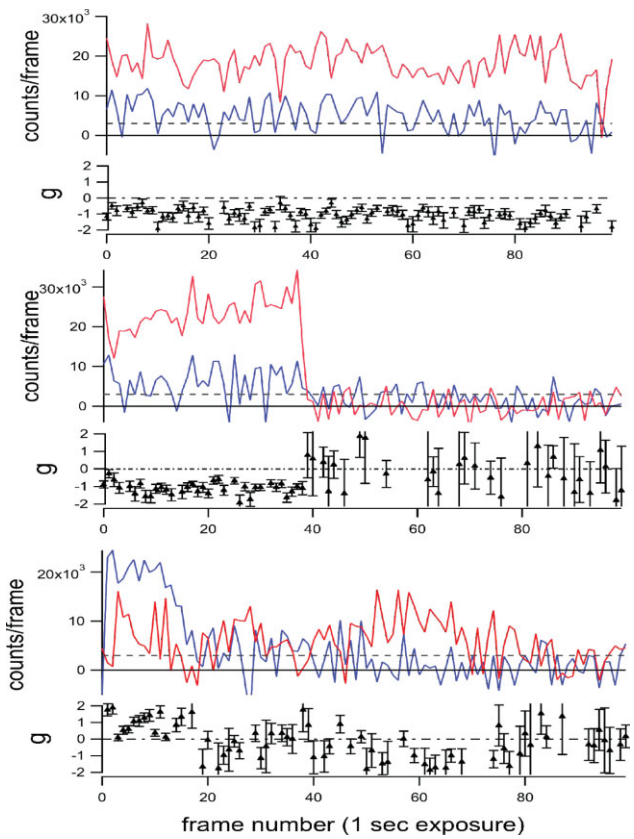

Fig. 6. Polarization-resolved intensity trajectories from different single P2 Helicene molecules (red = RCP, blue = LCP), and corresponding dissymmetry parameter trajectories. [Color figure can be viewed in the online issue, which is available at www.interscience.wiley.com.]

Summary

In this article, we have summarized our work on single-molecule radiation pattern imaging, fluorescence excitation, and circular-polarized emission dissymmetries using the bridged triaryl amine helicenes as prototype probe molecule. We believe there is a large molecular sample space yet to be explored that will reveal new information on the hidden heterogeneities of the chiroptical response in condensed phase. In addition, our future work will allow direct extraction of molecular frame orientation via emission pattern imaging and comparison with simulations. This, in turn, will provide the necessary components for a direct comparison with high-level theoretical calculations, and new insights into the role of local molecular environment and solvation on the single-molecule chiroptical response.

ACKNOWLEDGMENTS

The authors thank Jochen Autschbach, Jim Cheeseman, Robert Dickson, Nina Berova, Nathan Hammer, Bart Kahr, Mohan Srinivasarao, and Pat Vaccaro, for many helpful discussions.

LITERATURE CITED

1. Barron L. Molecular light scattering and optical activity, 2nd ed. Cambridge University Press; 2004.
2. Berova N, Nakanishi K, Woody RW, editors. Circular dichroism: principles and applications, 2nd ed. New York: Wiley-VCH; 2000.
3. Stephens PJ, Devlin FJ, Cheeseman JR, Frisch MJ. Calculation of optical rotation using density functional theory. J Phys Chem A 2001;105:5356–5371.
4. Cheeseman JR, Frisch MJ, Devlin FJ, Stephens PJ, Cammi R, Mennucci B, Tomasi J. Ab initio calculation of optical rotation. Abstr Pap Am Chem Soc 2000;219:U348–U348.
5. Ashvar CS, Devlin FJ, Stephens PJ. Molecular structure in solution: an ab initio vibrational spectroscopy study of phenyloxirane. J Am Chem Soc 1999;121:2836–2849.
6. Devlin FJ, Stephens PJ, Cheeseman JR, Frisch MJ. Ab initio prediction of vibrational absorption and circular dichroism spectra of chiral natural products using density functional theory: camphor and fenchone. J Phys Chem A 1997;101:6322–6333.
7. Nafie LA, Keiderling TA, Stephens PJ. Vibrational circular-dichroism. J Am Chem Soc 1976;98:2715–2723.
8. Wu CS, Ambler E, Hayward RW, Hoppes DD, Hudson RP. "Experimental test of parity conservation in beta-decay. Phys Rev 1957;105: 1413–1415.
9. Glashow SL, Weinberg S. Breaking chiral symmetry. Phys Rev Lett 1968;20:224–227.
10. Coleman S, Glashow SL. Chiral symmetries. Ann Phys 1962;17:41–60.
11. Allevi P, Cribiu R, Giannini E, Anastasia M. Practical syntheses of pyridinolines, important amino acidic biomarkers of collagen health. J Org Chem 2007;72:3478–3483.
12. Varghese OP, Barman J, Pathmasiri W, Plashkevych O, Honcharenko D, Chattopadhyaya J. Conformationally constrained 2′-N,4′-C-ethylene-bridged thymidine (aza-ENA-T): synthesis, structure, physical, and biochemical studies of aza-ENA-T-modified oligonucleotides. J Am Chem Soc 2006;128:15173–15187.
13. Ferber B, Top S, Vessieres A, Welter R, Jaouen G. Synthesis of optically pure o- formylcyclopentadienyl metal complexes of 17 alpha-ethynylestradiol. Recognition of the planar chirality by the estrogen receptor. Organometallics 2006;25:5730–5739.
14. Major DT, Nahum V, Wang YF, Reiser G, Fischer B. Molecular recognition in purinergic receptors. 2. Diastereoselectivity of the h-P2Y(1)-receptor. J Med Chem 2004;47:4405–4416.
15. Agmon I, Amit M, Auerbach T, Bashan A, Baram D, Bartels H, Berisio R, Greenberg I, Harms J, Hansen HAS, Kessler M, Pyetan E, Schluenzen F, Sittner A, Yonath A, Zarivach R. Ribosomal crystallography: a flexible nucleotide anchoring tRNA translocation facilitates peptide-bond formation, chirality discrimination and antibiotics synergism. FEBS Lett 2004;567:20–26.
16. Yashima E, Maeda K. Chirality-responsive helical polymers. Macromolecules 2008;41:3–12.
17. Wang W, Shaller AD, Li ADQ. "Twisted perylene stereodimers reveal chiral molecular assembly codes. J Am Chem Soc 2008;130: 8271–8279.
18. Izake EL. Chiral discrimination and enantioselective analysis of drugs: an overview. J Pharm Sci 2007;96:1659–1676.
19. Lemieux RP. Molecular recognition in chiral smectic liquid crystals: the effect of core core interactions and chirality transfer on polar order. Chem Soc Rev 2007;36:2033–2045.
20. Fasel R, Parschau M, Ernst KH. Amplification of chirality in two-dimensional enantiomorphous lattices. Nature 2006;439:449–452.
21. Guo PZ, Zhang L, Liu MH. A supramolecular chiroptical switch exclusively from an achiral amphiphile. Adv Mater 2006;18:177.
22. Seeber G, Tiedemann BEF, Raymond KN. Supramolecular chirality in coordination chemistry. Supramol Chirality 2006;265:147–183.
23. Miyauchi M, Takashima Y, Yamaguchi H, Harada A. Chiral supramolecular polymers formed by host-guest interactions. J Am Chem Soc 2005;127:2984–2989.
24. Zhang J, Albelda MT, Liu Y, Canary JW. Chiral nanotechnology. Chirality 2005;17:404–418.
25. Tamura K, Sato H, Yamashita S, Yamagishi A, Yamada H. Orientational tuning of monolayers of amphiphilic ruthenium(II) complexes for optimizing chirality distinction capability. J Phys Chem B 2004; 108:8287–8293.
26. van Delden RA, Huck NPM, Piet JJ, Warman JM, Meskers SCJ, Dekkers HPJM, Feringa BL. Remarkable solvent-dependent excited-state chirality: a molecular modulator of circularly polarized luminescence. J Am Chem Soc 2003;125:15659–15665.
27. Allenmark S. Induced circular dichroism by chiral molecular interaction. Chirality 2003;15:409–422.
28. Lahav M, Kharitonov AB, Willner I. Imprinting of chiral molecular recognition sites in thin TiO2 films associated with field-effect transistors: novel functionalized devices for chiroselective and chirospecific analyses. Chem Eur J 2001;7:3992–3997.
29. Huang XF, Nakanishi K, Berova N. Porphyrins and metalloporphyrins: versatile circular dichroic reporter groups for structural studies. Chirality 2000;12:237–255.
30. Rekharsky M, Inoue Y. Chiral recognition thermodynamics of beta-cyclodextrin: the thermodynamic origin of enantioselectivity and the enthalpy-entropy compensation effect. J Am Chem Soc 2000; 122:4418–4435.
31. Ryu JH, Tang L, Lee E, Kim HJ, Lee M. Supramolecular helical columns from the self- assembly of chiral rods. Chem Eur J 2008;14: 871–881.
32. Gottarelli G, Lena S, Masiero S, Pieraccini S, Spada GP. The use of circular dichroism spectroscopy for studying the chiral molecular self-assembly: an overview. Chirality 2008;20:471–485.
33. Dressler DH, Mastai Y. Chiral crystallization of glutamic acid on self assembled films of cysteine. Chirality 2007;19:358–365.
34. Rudick JG, Percec V. Helical chirality in dendronized polyarylacetylenes. New J Chem 2007;31:1083–1096.
35. De Feyter S, De Schryver FC. Two-dimensional supramolecular self-assembly probed by scanning tunneling microscopy. Chem Soc Rev 2003;32:139–150.
36. Fasel R, Parschau M, Ernst KH. Chirality transfer from single molecules into self- assembled monolayers. Angew Chem Int Ed 2003; 42:5178–5181.
37. Schenning APHJ, Kilbinger AFM, Biscarini F, Cavallini M, Cooper HJ, Derrick PJ, Feast WJ, Lazzaroni R, Leclere P, McDonell LA, Meijer EW, Meskers SCJ. Supramolecular organization of alpha,

alpha′-disubstituted sexithiophenes. J Am Chem Soc 2002;124:1269–1275.

38. Barth JV, Weckesser J, Trimarchi G, Vladimirova M, De Vita A, Cai CZ, Brune H, Gunter P, Kern K. Stereochemical effects in supramolecular self-assembly at surfaces: 1-D versus 2-D enantiomorphic ordering for PVBA and PEBA on Ag(111). J Am Chem Soc 2002; 124:7991–8000.
39. Li CJ, Zeng QD, Wu P, Xu SL, Wang C, Qiao YH, Wan LJ, Bai CL. Molecular symmetry breaking and chiral expression of discotic liquid crystals in two-dimensional systems. J Phys Chem B 2002;106: 13262–13267.
40. Kirstein S, von Berlepsch H, Bottcher C, Burger C, Ouart A, Reck G, Dahne S. Chiral J-aggregates formed by achiral cyanine dyes. Chemphyschem 2000;1:146.
41. Engelkamp H, Middelbeek S, Nolte RJM. Self-assembly of disk-shaped molecules to coiled-coil aggregates with tunable helicity. Science 1999;284:785–788.
42. Prins LJ, Huskens J, de Jong F, Timmerman P, Reinhoudt DN. Complete asymmetric induction of supramolecular chirality in a hydrogen-bonded assembly. Nature 1999;398:498–502.
43. Charra F, Cousty J. Surface-induced chirality in a self-assembled monolayer of discotic liquid crystal. Phys Rev Lett 1998;80:1682–1685.
44. Spector MS, Easwaran KRK, Jyothi G, Selinger JV, Singh A, Schnur JM. Chiral molecular self-assembly of phospholipid tubules: a circular dichroism study. Proc Natl Acad Sci USA 1996;93:12943–12946.
45. Hanessian S, Simard M, Roelens S. Molecular recognition and self-assembly by non-amidic hydrogen-bonding—an exceptional assembler of neutral and charged supramolecular structures. J Am Chem Soc 1995;117:7630–7645.
46. Brienne MJ, Gabard J, Leclercq M, Lehn JM, Cesario M, Pascard C, Cheve M, Dutrucrosset G. Chirality directed self-assembly—resolution of 2,5-diazabicyclo[2.2.2]octane-3,6-dione and crystal-structures of its racemic and (−) enantiomeric Forms. Tetrahedron Lett 1994;35:8157–8160.
47. Selinger JV, Schnur JM. Theory of chiral lipid tubules. Phys Rev Lett 1993;71:4091–4094.
48. Schnur JM. Lipid tubules—a paradigm for molecularly engineered structures. Science 1993;262:1669–1676.
49. Ashton PR, Brown GR, Isaacs NS, Giuffrida D, Kohnke FH, Mathias JP, Slawin AMZ, Smith DR, Stoddart JF, Williams DJ. Molecular lego. I. Substrate-directed synthesis via stereoregular Diels-Alder oligomerizations. J Am Chem Soc 1992;114:6330–6353.
50. Srinivasarao M. Chirality and polymers. Curr Opin Colloid Interface Sci 1999;4:147–152.
51. Autschbach J, Jensen L, Schatz GC, Tse YCE, Krykunov M. Time-dependent density functional calculations of optical rotatory dispersion including resonance wavelengths as a potentially useful tool for determining absolute configurations of chiral molecules. J Phys Chem A 2006;110:2461–2473.
52. Wilson SM, Wiberg KB, Cheeseman JR, Frisch MJ, Vaccaro PH. Nonresonant optical activity of isolated organic molecules. J Phys Chem A 2005;109:11752–11764.
53. Cantuel M, Bernardinelli G, Muller G, Riehl JP, Piguet C. The first enantiomerically pure helical noncovalent tripod for assembling nine-coordinate lanthanide(III) podates. Inorg Chem 2004;43:1840–1849.
54. Muller T, Wiberg KB, Vaccaro PH, Cheeseman JR, Frisch MJ. Cavity ring-down polarimetry (CRDP): theoretical and experimental characterization. J Opt Soc Am B 2002;19:125–141.
55. Kuball HG, Altschuh J. Optical-activity of oriented molecules. 7. Comparison of the optical-rotatory dispersion and the circular-dichroism through the Kramers Kronig transform. Chem Phys Lett 1982;87:599–603.
56. Kaminsky W, Geday MA, Herreros-Cedres J, Kahr B. Optical rotatory and circular dichroic scattering. J Phys Chem A 2003;107:2800–2807.
57. Tanaka K, Pescitelli G, Nakanishi K, Berova N. Fluorescence detected exciton coupled circular dichroism: development of new fluorescent reporter groups for structural studies. Monatsh Chem 2005;136:367–395.
58. Nehira T, Tanaka K, Takakuwa T, Ohshima C, Masago H, Pescitelli G, Wada A, Berova N. Development of a universal ellipsoidal mirror device for fluorescence detected circular dichroism: elimination of polarization artifacts. Appl Spectrosc 2005;59:121–125.
59. Muller G, Muller FC, Maupin CL, Riehl JP. The measurement of the fluorescence detected circular dichroism (FDCD) from a chiral Eu(III) system. Chem Commun 2005;28:3615–3617.
60. Nehira T, Parish CA, Jockusch S, Turro NJ, Nakanishi K, Berova N. Fluorescence- detected exciton-coupled circular dichroism: scope and limitation in structural studies of organic molecules. J Am Chem Soc 1999;121:8681–8691.
61. Dong JG, Wada A, Takakuwa T, Nakanishi K, Berova N. Sensitivity enhancement of exciton coupling by fluorescence detected circular dichroism (FDCD). J Am Chem Soc 1997;119:12024–12025.
62. Lamos ML, Lobenstine EW, Turner DH. Fluorescence-detected circular-dichroism of ethidium bound to nucleic-acids. J Am Chem Soc 1986;108:4278–4284.
63. Lamos ML, Walker GT, Krugh TR, Turner DH. Fluorescence-detected circular- dichroism of ethidium bound to Poly(Dg-Dc) and Poly(Dg-M5dc) under B-Form and Z-Form conditions. Biochemistry 1986;25:687–691.
64. Lamos ML, Walker GT, Krugh TR, Turner DH. Fluorescence-detected circular-dichroism of ethidium invivo and bound to nucleic-acids invitro. J Electrochem Soc 1985;132:C365–C365.
65. Lobenstine EW, Schaefer WC, Turner DH. Fluorescence detected circular-dichroism of proteins with single fluorescent tryptophans. J Am Chem Soc 1981;103:4936–4940.
66. Lobenstine EW, Turner DH. Further verification of fluorescence-detected circular- dichroism. J Am Chem Soc 1980;102:7786–7787.
67. Lobenstine EW, Turner DH. Photo-selected fluorescence detected circular-dichroism. J Am Chem Soc 1979;101:2205–2207.
68. Tinoco I, Ehrenberg B, Steinberg IZ. Fluorescence detected circular-dichroism and circular-polarization of luminescence in rigid media—direction dependent optical-activity obtained by photoselection. J Chem Phys 1977;66:916–920.
69. Ehrenberg B, Steinberg IZ. Effect of photoselection on fluorescence-detected circular- dichroism. J Am Chem Soc 1976;98:1293–1295.
70. Tinoco I, Turner DH. Fluorescence detected circular-dichroism—theory. J Am Chem Soc 1976;98:6453–6456.
71. Turner DH, Tinoco I, Maestre M. Fluorescence detected circular-dichroism. J Am Chem Soc 1974;96:4340–4342.
72. McCann DM, Stephens PJ. Determination of absolute configuration using density functional theory calculations of optical rotation and electronic circular dichroism: chiral alkenes. J Org Chem 2006;71: 6074–6098.
73. Stephens PJ, McCann DM, Devlin FJ, Smith AB. Determination of the absolute configurations of natural products via density functional theory calculations of optical rotation, electronic circular dichroism, and vibrational circular dichroism: the cytotoxic sesquiterpene natural products quadrone, suberosenone, suberosanone, and suberosenol A acetate. J Nat Prod 2006;69:1055–1064.
74. Devlin FJ, Stephens PJ, Bortolini O. Determination of absolute configuration using vibrational circular dichroism spectroscopy: phenyl glycidic acid derivatives obtained via asymmetric epoxidation using oxone and a keto bile acid. Tetrahedron: Asymmetry 2005;16:2653–2663.
75. Stephens PJ, McCann DM, Cheeseman JR, Frisch MJ. Determination of absolute configurations of chiral molecules using ab initio time-dependent density functional theory calculations of optical rotation: how reliable are absolute configurations obtained for molecules with small rotations? Chirality 2005;17:S52–S64.
76. Urbanova M, Setnicka V, Devlin FJ, Stephens PJ. Determination of molecular structure in solution using vibrational circular dichroism spectroscopy: the supramolecular tetramer of S-2,2′-dimethyl-biphenyl-6,6′-dicarboxylic acid. J Am Chem Soc 2005;127:6700–6711.

77. Stephens PJ, McCann DM, Devlin FJ, Flood TC, Butkus E, Stoncius S, Cheeseman JR. Determination of molecular structure using vibrational circular dichroism spectroscopy: the keto-lactone product of Baeyer-Villiger oxidation of (+)-(1R,5S)-bicyclo[3.3.1]nonane-2,7-dione. J Org Chem 2005;70:3903–3913.
78. Devlin FJ, Stephens PJ, Besse P. Are the absolute configurations of 2-(1-hydroxyethyl)- chromen-4-one and its 6-bromo derivative determined by X-ray crystallography correct? A vibrational circular dichroism study of their acetate derivatives. Tetrahedron: Asymmetry 2005;16:1557–1566.
79. Devlin FJ, Stephens PJ, Besse P. Conformational rigidification via derivatization facilitates the determination of absolute configuration using chiroptical spectroscopy: a case study of the chiral alcohol endo-borneol. J Org Chem 2005;70:2980–2993.
80. Cere V, Peri F, Pollicino S, Ricci A, Devlin FJ, Stephens PJ, Gasparrini F, Rompietti R, Villani C. Synthesis, chromatographic separation, vibrational circular dichroism spectroscopy, and a initio DFT studies of chiral thiepane tetraol derivatives. J Org Chem 2005;70: 664–669.
81. McCann DM, Stephens PJ, Cheeseman JR. Determination of absolute configuration using density functional theory calculation of optical rotation: chiral Alkanes. J Org Chem 2004;69:8709–8717.
82. Stephens PJ, McCann DM, Butkus E, Stoncius S, Cheeseman JR, Frisch MJ. Determination of absolute configuration using concerted ab initio DFT calculations of electronic circular dichroism and optical rotation: bicyclo[3.3.1]nonane diones. J Org Chem 2004;69: 1948–1958.
83. Hassey R, Swain EJ, Hammer NI, Venkataraman D, Barnes MD. Probing the chiroptical response of a single molecule. Science 2006; 314:1437–1439.
84. Pedersen TB, Hansen AE. Ab-initio calculation and display of the rotatory strength tensor in the random-phase-approximation—method and model studies. Chem Phys Lett 1995;246:1–8.
85. Claborn K, Chu AS, Jang SH, Su FY, Kaminsky W, Kahr B. Circular extinction imaging: determination of the absolute orientation of embedded chromophores in enantiomorphously twinned LiKSO4 crystals. Cryst Growth Des 2005;5:2117–2123.
86. Wustholz KL, Kahr B, Reid PJ. Single-molecule orientations in dyed salt crystals. J Phys Chem B 2005;109:16357–16362.
87. Kaminsky W, Claborn K, Kahr B. Polarimetric imaging of crystals. Chem Soc Rev 2004;33:514–525.
88. Claborn K, Puklin-Faucher E, Kurimoto M, Kaminsky W, Kahr B. Circular dichroism imaging microscopy: application to enantiomorphous twinning in biaxial crystals of 1,8-dihydroxyanthraquinone. J Am Chem Soc 2003;125:14825–14831.
89. Stockman TG, Klevickis CA, Grisham CM, Richardson FS. Intermolecular chiral recognition probed by enantiodifferential excited-state quenching kinetics. J Mol Recognit 1996;9:595–606.
90. Riehl JP, Richardson FS. Circularly-polarized luminescence. Metallobiochem C 1993;226:539–553.
91. Metcalf DH, Snyder SW, Wu SG, Hilmes GL, Riehl JP, Demas JN, Richardson FS. Excited–state chiral discrimination observed by time–resolved circularly polarized luminescence measurements. J Am Chem Soc 1989;111:3082–3083.
92. Riehl JP, Richardson FS. Circularly polarized luminescence spectroscopy. Chem Rev 1986;86:1–16.
93. Riehl JP, Richardson FS. Polarization of pure electric quadrupole transitions in the electronic-spectra of molecules. J Chem Phys 1980;72:2138–2147.
94. Boyd DB, Riehl JP, Richardson FS. Electronic-structures of cephalosporins and penicillins. 8. Chiroptical properties of 1-Carbapenam and orbital mixing in nonplanar amides. Tetrahedron 1979;35:1499–1508.
95. Riehl JP, Richardson FS. Theory of magnetic linearly polarized emission. I. paramagnetic molecules in a rigid isotropic medium. J Chem Phys 1978;68:4266–4275.
96. Richardson FS, Riehl JP. Circularly polarized luminescence spectroscopy. Chem Rev 1977;77:773–792.
97. Thompson LC, Serra OA, Riehl JP, Richardson FS, Schwartz RW. Emission-spectra of Cs2natbcl6 and Cs2naycl6-Tb3+. Chem Phys 1977;26:393–401.
98. Schwartz RW, Brittain HG, Riehl JP, Yeakel W, Richardson FS. Magnetic circularly polarized emission and magnetic circular-dichroism study of F-7(J)reversible D-5(4) transitions in crystalline Cs2natbcl6. Mol Phys 1977;34:361–379.
99. Riehl JP, Richardson FS. Theory of magnetic circularly polarized emission. J Chem Phys 1977;66:1988–1998.
100. Riehl JP, Richardson FS. Determination of vibrational and orientational time-correlation functions from Raman-scattering of circularly polarized-light. Chem Phys Lett 1976;42:501–505.
101. Riehl JP, Richardson FS. General theory of circularly polarized emission and magnetic circularly polarized emission from molecular systems. J Chem Phys 1976;65:1011–1021.
102. Isborn C, Claborn K, Kahr B. The optical rotatory power of water. J Phys Chem A 2007;111:7800–7804.
103. Wiberg KB, Wang YG, Wilson SM, Vaccaro PH, Jorgensen WL, Crawford TD, Abrams ML, Cheeseman JR, Luderer M. Optical rotatory dispersion of 2,3-hexadiene and 2,3- pentadiene. J Phys Chem A 2008;112:2415–2422.
104. Wilson SM, Wiberg KB, Murphy MJ, Vaccaro PH. The effects of conformation and solvation on optical rotation: substituted epoxides. Chirality 2008;20:357–369.
105. Eelkema R, Feringa BL. Amplification of chirality in liquid crystals. Org Biomol Chem 2006;4:3729–3745.
106. Wiberg KB, Wang YG, Wilson SM, Vaccaro PH, Cheeseman JR. Chiroptical properties of 2-chloropropionitrile. J Phys Chem A 2005; 109:3448–3453.
107. Wiberg KB, Wang YG, Vaccaro PH, Cheeseman JR, Luderer MR. Conformational effects on optical rotation. 2-Substituted butanes. J Phys Chem A 2005;109:3405–3410.
108. Wiberg KB, Wang Y, de Oliveira AE, Perera SA, Vaccaro PH. Comparison of CIS- and EOM-CCSD-calculated adiabatic excited-state structures. Changes in charge density on going to adiabatic excited states. J Phys Chem A 2005;109:466–477.
109. Wiberg KB, Wang YG, Murphy MJ, Vaccaro PH. Temperature dependence of optical rotation: alpha-pinene, beta-pinene pinane, camphene, camphor and fenchone. J Phys Chem A 2004;108:5559–5563.
110. Wiberg KB, Wang YG, Vaccaro PH, Cheeseman JR, Trucks G, Frisch MJ. Optical activity of 1-butene, butane, and related hydrocarbons. J Phys Chem A 2004;108:32–38.
111. Wiberg KB, Vaccaro PH, Cheeseman JR. Conformational effects on optical rotation. 3-Substituted 1-butenes. J Am Chem Soc 2003;125: 1888–1896.
112. Muller T, Wiberg KB, Vaccaro PH. An optical mounting system for cavity ring-down polarimetry. Rev Sci Instrum 2002;73:1340–1342.
113. Muller T, Wiberg KB, Vaccaro PH. Cavity ring-down polarimetry (CRDP): a new scheme for probing circular birefringence and circular dichroism in the gas phase. J Phys Chem A 2000;104:5959–5968.
114. Kongsted J, Ruud K. Solvent effects on zero-point vibrational corrections to optical rotations and nuclear magnetic resonance shielding constants. Chem Phys Lett 2008;451:226–232.
115. Kongsted J, Mennucci B. How to model solvent effects on molecular properties using quantum chemistry? Insights from polarizable discrete or continuum solvation models. J Phys Chem A 2007;111: 9890–9900.
116. Kongsted J, Pedersen TB, Jensen L, Hansen AE, Mikkelsen KV. Coupled cluster and density functional theory studies of the vibrational contribution to the optical rotation of (S)-propylene oxide. J Am Chem Soc 2006;128:976–982.
117. Kongsted J, Pedersen TB, Strange M, Osted A, Hansen AE, Mikkelsen KV, Pawlowski F, Jorgensen P, Hattig C. Coupled cluster calculations of the optical rotation of S-propylene oxide in gas phase and solution. Chem Phys Lett 2005;401:385–392.
118. Osted A, Kongsted J, Christiansen O. Theoretical study of the electronic gas-phase spectrum of glycine, alanine, and related amines and carboxylic acids. J Phys Chem A 2005;109:1430–1440.

119. Kongsted J, Hansen AE, Pedersen TB, Osted A, Mikkelsen KV, Christiansen O. A coupled cluster study of the oriented circular dichroism of the n ->pi* electronic transition in cyclopropanone and natural optical active related structures. Chem Phys Lett 2004;391: 259–266.

120. Kongsted J, Pedersen TB, Osted A, Hansen AE, Mikkelsen KV, Christiansen O. Solvent effects on rotatory strength tensors. 1. Theory and application of the combined coupled cluster/dielectric continuum model. J Phys Chem A 2004;108:3632–3641.

121. Kongsted J, Osted A, Mikkelsen KV, Astrand PO, Christiansen O. Solvent effects on the n ->pi(*) electronic transition in formaldehyde: a combined coupled cluster/molecular dynamics study. J Chem Phys 2004;121:8435–8445.

122. Crawford TD, Stephens PJ. Comparison of time-dependent density-functional theory and coupled cluster theory for the calculation of the optical rotations of chiral molecules. J Phys Chem A 2008;112: 1339–1345.

123. Crawford TD, Tam MC, Abrams ML. The problematic case of (S)-methylthiirane: electronic circular dichroism spectra and optical rotatory dispersion. Mol Phys 2007;105:2607–2617.

124. Crawford TD, Tam MC, Abrams ML. The current state of ab initio calculations of optical rotation and electronic circular dichroism spectra. J Phys Chem A 2007;111:12057–12068.

125. Tam MC, Abrams ML, Crawford TD. Chiroptical properties of (R)-3-chloro-l-butene and (R)-2-chlorobutane. J Phys Chem A 2007;111: 11232–11241.

126. Kowalczyk TD, Abrams ML, Crawford TD. Ab initio optical rotatory dispersion and electronic circular dichroism spectra of (S)-2-chloropropionitrile. J Phys Chem A 2006;110:7649–7654.

127. Crawford TD. Ab initio calculation of molecular chiroptical properties. Theor Chem Acc 2006;115:227–245.

128. Carlier PR, Deora N, Crawford TD. Protonated 2-methyl-1,2-epoxypropane: a challenging problem for density functional theory. J Org Chem 2006;71:1592–1597.

129. Le Guennic B, Hieringer W, Gorling A, Autschbach J. Density functional calculation of the electronic circular dichroism spectra of the transition metal complexes [M(phen)(3)](2+) (M = Fe, Ru, Os). J Phys Chem A 2005;109:4836–4846.

130. Autschbach J, Jorge FE, Zlegler T. Density functional calculations on electronic circular dichroism spectra of chiral transition metal complexes. Inorg Chem 2003;42:2867–2877.

131. Autschbach J, Ziegler T, van Gisbergen SJA, Baerends EJ. Chiroptical properties from time-dependent density functional theory. I. Circular dichroism spectra of organic molecules. J Chem Phys 2002; 116:6930–6940.

132. Autschbach J, Patchkovskii S, Ziegler T, van Gisbergen SJA, Baerends EJ. Chiroptical properties from time-dependent density functional theory. II. Optical rotations of small to medium sized organic molecules. J Chem Phys 2002;117:581–592.

133. Autschbach J, Ziegler T. Density functional implementation of the computation of chiroptical molecular properties. Abstr Pap Am Chem Soc 2001;222:U405–U405.

134. Prince RB, Brunsveld L, Meijer EW, Moore JS. Twist sense bias induced by chiral side chains in helically folded oligomers. Angew Chem Int Ed 2000;39:228.

135. Gin MS, Yokozawa T, Prince RB, Moore JS. Helical bias in solvophobically folded oligo(phenylene ethynylene)s. J Am Chem Soc 1999;121:2643–2644.

136. Wilson JN, Steffen W, McKenzie TG, Lieser G, Oda M, Neher D, Bunz UHF. Chiroptical properties of poly(p-phenyleneethynylene) copolymers in thin films: large g-values. J Am Chem Soc 2002;124: 6830–6831.

137. Muller G, Mamula I, Imbert D, Bunzli JCG, Murner HR, Riehl JP. Photophysical and chiroptical properties of lanthanide triple helical complexes with a terdentate chiral C-2 symmetric ligand. Abstr Pap Am Chem Soc 2003;226:U706–U706.

138. Satrijo A, Swager TM. Facile control of chiral packing in poly(p-phenylenevinylene) spin-cast films. Macromolecules 2005;38:4054–4057.

139. Jones TV, Slutsky MM, Laos R, de Greef TFA, Tew GN. Solution H-1 NMR confirmation of folding in short o-phenylene ethynylene oligomers. J Am Chem Soc 2005;127:17235–17240.

140. Stowe AC, Nellutla S, Dalal NS, Kortz U. Magnetic properties of lone-pair-containing, sandwich-type polyoxoanions: a detailed study of the heteroatomic effect. Eur J Inorg Chem 2004;19:3792–3797.

141. Arnt L, Tew GN. Conformational changes of facially amphiphilic meta-poly(phenylene ethynylene)s in aqueous solution. Macromolecules 2004;37:1283–1288.

142. Blatchly RA, Tew GN. Theoretical study of helix formation in substituted phenylene ethynylene oligomers. J Org Chem 2003;68:8780–8785.

143. Moerner WE. A dozen years of single-molecule spectroscopy in physics, chemistry, and biophysics. J Phys Chem B 2002;106:910–927.

144. Yang H, Xie XS. Probing single-molecule dynamics photon by photon. J Chem Phys 2002;117:10965–10979.

145. Yang H, Xie XS. Statistical approaches for probing single-molecule dynamics photon-by-photon. Chem Phys 2002;284:423–437.

146. Xie XS, Trautman JK. Optical studies of single molecules at room temperature. Annu Rev Phys Chem 1998;49:441–480.

147. Nie SM, Zare RN. Optical detection of single molecules. Annu Rev Biophys Biomol Struct 1997;26:567–596.

148. Brokmann X, Coolen L, Dahan M, Hermier JP. Measurement of the radiative and nonradiative decay rates of single CdSe nanocrystals through a controlled modification of their spontaneous emission. Phys Rev Lett 2004;93.

149. Moerner WE, Fromm DP. Methods of single-molecule fluorescence spectroscopy and microscopy. Rev Sci Instrum 2003;74:3597–3619.

150. Hernando J, van der Schaaf M, van Dijk EMHP, Sauer M, Garcia-Parajo MF, van Hulst NF. Excitonic behavior of rhodamine dimers: a single-molecule study. J Phys Chem A 2003;107:43–52.

151. Hammer NI, Early KT, Sill K, Odoi MY, Emrick T, Barnes MD. Coverage-mediated suppression of blinking in solid state quantum dot conjugated organic composite nanostructures. J Phys Chem B 2006;110:14167–14171.

152. Odoi MY, Hammer NI, Sill K, Emrick T, Barnes MD. Observation of enhanced energy transfer in individual quantum dot-oligophenylene vinylene nanostructures. J Am Chem Soc 2006;128:3506–3507.

153. Yokota H, Ishii Y, Yanagida T. Blinking and its effect on single molecule FRET measurements. Biophys J 2001;80:150A–150A.

154. Cao JS. Single molecule waiting time distribution functions in quantum processes. J Chem Phys 2001;114:5137–5140.

155. Kuno M, Fromm DP, Hamann HF, Gallagher A, Nesbitt DJ. Nonexponential "blinking" kinetics of single CdSe quantum dots: a universal power law behavior. J Chem Phys 2000;112:3117–3120.

156. Barnes MD, Mehta A, Thundat T, Bhargava RN, Chhabra V, Kulkarni B. On-off blinking and multiple bright states of single europium ions in Eu3+: Y2O3 nanocrystals. J Phys Chem B 2000;104: 6099–6102.

157. Stracke F, Blum C, Becker S, Mullen K, Meixner AJ. Intrinsic conformer jumps observed by single molecule spectroscopy in real time. Chem Phys Lett 2000;325:196–202.

158. Neuhauser RG, Shimizu KT, Woo WK, Empedocles SA, Bawendi MG. Correlation between fluorescence intermittency and spectral diffusion in single semiconductor quantum dots. Phys Rev Lett 2000;85:3301–3304.

159. Krauss TD, Brus LE. Charge, polarizability, and photoionization of single semiconductor nanocrystals. Phys Rev Lett 1999;83:4840–4843.

160. Bertram D, Hanna MC, Nozik AJ. Two color blinking of single strain-induced GaAs quantum dots. Appl Phys Lett 1999;74:2666–2668.

161. Jung G, Wiehler J, Gohde W, Tittel J, Basche T, Steipe B, Brauchle C. Confocal microscopy of single molecules of the green fluorescent protein. Bioimaging 1998;6:54–61.

162. Gohde W, Fischer UC, Fuchs H, Tittel J, Basche T, Brauchle C, Herrmann A, Mullen K. Fluorescence blinking and photobleaching

of single terrylenediimide molecules studied with a confocal microscope. J Phys Chem A 1998;102:9109–9116.

163. Dickson RM, Cubitt AB, Tsien RY, Moerner WE. On/off blinking and switching behaviour of single molecules of green fluorescent protein. Nature 1997;388:355–358.
164. He Y, Barkai E. Influence of spectral diffusion on single-molecule photon statistics. Phys Rev Lett 2004;93.
165. Andersen PC, Jacobson ML, Rowlen KL. Flashy silver nanoparticles. J Phys Chem B 2004;108:2148–2153.
166. Kumar P, Mehta A, Dadmun MD, Zheng J, Peyser L, Bartko AP, Dickson RM, Thundat T, Sumpter BG, Noid DW, Barnes MD. Narrow-bandwidth spontaneous luminescence from oriented semiconducting polymer nanostructures. J Phys Chem B 2003;107:6252–6257.
167. Svishchev GM. Photon correlation probing of spectral diffusion in impurity glasses. Opt Spectrosc 2003;95:933–937.
168. Hofmann C, Aartsma TJ, Michel H, Kohler J. Direct observation of tiers in the energy landscape of a chromoprotein: a single-molecule study. Proc Natl Acad Sci USA 2003;100:15534–15538.
169. Suh YD, Schenter GK, Zhu LY, Lu HP. Probing nanoscale surface enhanced Raman-scattering fluctuation dynamics using correlated AFM and confocal ultramicroscopy. Ultramicroscopy 2003;97:89–102.
170. Mulvaney SP, Musick MD, Keating CD, Natan MJ. Glass-coated, analyte-tagged nanoparticles: a new tagging system based on detection with surface-enhanced Raman scattering. Langmuir 2003;19:4784–4790.
171. Osad'ko IS, Khots EV. Fluctuating absorption coefficient of single molecule. J Lumin 2003;102:581–585.
172. Orrit M. Photon statistics in single molecule experiments. Single Mol 2002;3:255–265.
173. Orrit M. Single-molecule spectroscopy: the road ahead. J Chem Phys 2002;117:10938–10946.
174. Osad'ko IS, Khots EV. Scan time dependence of single molecule optical lines in polymers and glasses. Single Mol 2002;3:236–246.
175. Higgins DA, Collinson MM, Saroja G, Bardo AM. Single-molecule spectroscopic studies of nanoscale heterogeneity in organically modified silicate thin films. Chem Mater 2002;14:3734–3744.
176. Kuno M, Fromm DP, Hamann HF, Gallagher A, Nesbitt DJ. "On/off" fluorescence intermittency of single semiconductor quantum dots. J Chem Phys 2001;115:1028–1040.
177. Tietz C, Jelezko F, Gerken U, Schuler S, Schubert A, Rogl H, Wrachtrup J. Single molecule spectroscopy on the light-harvesting complex II of higher plants. Biophys J 2001;81:556–562.
178. English DS, Harbron EJ, Barbara PF. Role of rare sites in single molecule spectroscopy measurements of spectral diffusion. J Chem Phys 2001;114:10479–10485.
179. Naumov AV, Vainer YG, Bauer M, Zilker S, Kador L. Distributions of moments of single-molecule spectral lines and the dynamics of amorphous solids. Phys Rev B 2001;6321.
180. Leontidis E, Heinz H, Palewska K, Wallenborn EU, Suter UW. Normal and defective perylene substitution sites in alkane crystals. J Chem Phys 2001;114:3224–3235.
181. Donley EA, Plakhotnik T. Spectral diffusion in polyethylene: single-molecule studies performed between 30 mK and 1.8 K. J Chem Phys 2000;113:9294–9299.
182. Barkai E, Silbey R, Zumofen G. Transition from simple to complex behavior of single molecule line shapes in disordered condensed phase. J Chem Phys 2000;113:5853–5867.
183. Lazonder K, Duppen K, Wiersma DA. Ethanol glass dynamics: logarithmic line broadening and optically induced dephasing. J Phys Chem B 2000;104:6468–6477.
184. Zumofen G, Bach H, Renn A, Wild UP. Triplet-exciton dynamics in solid naphthalene investigated by single molecule spectroscopy. J Mol Liq 2000;86:183–192.
185. Barkai E, Silbey R, Zumofen G. Levy distribution of single molecule line shape cumulants in glasses. Phys Rev Lett 2000;84:5339–5342.
186. Osad'ko IS, Yershova LB. Exponential and logarithmic spectral diffusion in single molecule fluorescence. J Chem Phys 2000;112:9645–9654.
187. Donley EA, Bonsma S, Palm V, Burzomato V, Wild UP, Plakhotnik T. Zero-phonon lines of single molecules in polyethylene down to millikelvin temperatures. J Lumin 2000;87–89:109–114.
188. Osad'ko IS, Yershova LB. One- and two-photon counting methods in single molecule fluorescence. J Lumin 2000;87–89:184–188.
189. Plakhotnik T, Donley EA. Statistics of a single terrylene molecule in hexadecane. J Lumin 2000;86:175–180.
190. Meixner AJ, Weber MA. Single molecule spectral dynamics at room temperature. J Lumin 2000;86:181–187.
191. Palm V, Rebane K. On the role of spectral diffusion in single-molecule spectroscopy. J Lumin 2000;86:207–209.
192. Osad'ko IS, Yershova LB. Dynamical theory for two-photon correlators: spectral line jumps and spectral diffusion. J Lumin 2000;86:211–217.
193. Rothenberg E, Ebenstein Y, Kazes M, Banin U. Two-photon fluorescence microscopy of single semiconductor quantum rods: direct observation of highly polarized nonlinear absorption dipole. J Phys Chem B 2004;108:2797–2800.
194. Yanagida T, Ueda M, Murata T, Esaki S, Ishii Y. Brownian motion, fluctuation and life. Biosystems 2007;88:228–242.
195. Kim TG, Castro JC, Loudet A, Jiao JGS, Hochstrasser RM, Burgess K, Topp MR. Correlations of structure and rates of energy transfer for through-bond energy-transfer cassettes. J Phys Chem A 2006;110:20–27.
196. Mehta A, Kumar P, Dadmun MD, Zheng J, Dickson RM, Thundat T, Sumpter BG, Barnes MD. Oriented nanostructures from single molecules of a semiconducting polymer: polarization evidence for highly aligned intramolecular geometries. Nano Lett 2003;3:603–607.
197. Farrer RA, Previte MJR, Olson CE, Peyser LA, Fourkas JT, So PTC. Single- molecule detection with a two-photon fluorescence microscope with fast-scanning capabilities and polarization sensitivity. Opt Lett 1999;24:1832–1834.
198. Lermer N, Barnes MD, Kung CY, Whitten WB, Ramsey JM, Hill SC. Spatial photoselection of single molecules on the surface of spherical microcavities. Opt Lett 1998;23:951–953.
199. Schutz GJ, Schindler H, Schmidt T. Imaging single-molecule dichroism. Opt Lett 1997;22:651–653.
200. Wild UP, Croci M, Guttler F, Pirotta M, Renn A. Single-molecule spectroscopy—stark-polarization, pressure-polarization, polarization-effects and fluorescence lifetime measurements. J Lumin 1994;60–61:1003–1007.
201. Xie XS, Dunn RC. Probing single-molecule dynamics. Science 1994;265:361–364.
202. Kempa T, Farrer RA, Giersig M, Fourkas JT. Photochemical synthesis and multiphoton luminescence of monodisperse silver nanocrystals. Plasmonics 2006;1:45–51.
203. Steinmeyer R, Noskov A, Krasel C, Weber I, Dees C, Harms GS. Improved fluorescent proteins for single-molecule research in molecular tracking and co-localization. J Fluoresc 2005;15:707–721.
204. Mattheyses AL, Axelrod D. Fluorescence emission patterns near glass and metal-coated surfaces investigated with back focal plane imaging. J Biomed Opt 2005;10.
205. Brokmann X, Coolen L, Hermier JP, Dahan M. Emission properties of single CdSe/ZnS quantum dots close to a dielectric interface. Chem Phys 2005;318:91–98.
206. Osborne MA. Real-time dipole orientational imaging as a probe of ligand-protein interactions. J Phys Chem B 2005;109:18153–18161.
207. Zhou Q. Probing three-dimensional single-molecule rotational diffusion in polymer. J Korean Phys Soc 2005;47:S190–S193.
208. Schroeyers W, Vallee R, Patra D, Hofkens J, Habuchi S, Vosch T, Cotlet M, Mullen K, Enderlein J, De Schryver FC. Fluorescence lifetimes and emission patterns probe the 3D orientation of the emitting chromophore in a multichromophoric system. J Am Chem Soc 2004;126:14310–14311.

209. Patra D, Gregor I, Enderlein J. Image analysis of defocused single-molecule images for three-dimensional molecule orientation studies. J Phys Chem A 2004;108:6836–6841.

210. Lieb MA, Zavislan JM, Novotny L. Single-molecule orientations determined by direct emission pattern imaging. J Opt Soc Am B 2004;21:1210–1215.

211. Alivisatos P. The use of nanocrystals in biological detection. Nat Biotechnol 2004;22:47–52.

212. Webster G, Hilgenfeld R. Perspectives on single molecule diffraction using the x-ray free electron laser. Single Mol 2002;3:63–68.

213. Bartko AP, Dickson RM. Imaging three-dimensional single molecule orientations. J Phys Chem B 1999;103:11237–11241.

214. Bartko AP, Dickson RM. Three-dimensional orientations of polymer-bound single molecules. J Phys Chem B 1999;103:3053–3056.

215. Moerner WE, Kador L. Optical-detection and spectroscopy of single molecules in a solid. Phys Rev Lett 1989;62:2535–2538.

216. Ambrose WP, Basche T, Moerner WE. Detection and spectroscopy of single pentacene molecules in a para-terphenyl crystal by means of fluorescence excitation. J Chem Phys 1991;95:7150–7163.

217. Lakowicz JR. Principles of fluorescence spectroscopy, 3rd ed. Singapore: Springer; 2006.

218. Odoi MY, Hammer NI, Early KT, McCarthy KD, Tangirala R, Emrick T, Barnes MD. Fluorescence lifetimes and correlated photon statistics from single CdSe/oligo(phenylene vinylene) composite nanostructures. Nano Lett 2007;7:2769–2773.

219. Odoi MY, Hammer NI, Rathnayake HP, Lahti PM, Barnes MD. Single-molecule studies of a model fluorenone. Chemphyschem 2007;8:1481–1486.

220. Field JE, Hill TJ, Venkataraman D. Bridged triarylamines: a new class of heterohelicenes. J Org Chem 2003;68:6071–6078.

221. Field JE, Muller G, Riehl JP, Venkataraman D. Circularly polarized luminescence from bridged triarylamine helicenes. J Am Chem Soc 2003;125:11808–11809.

222. Bartko AP, Xu KW, Dickson RM. Three-dimensional single molecule rotational diffusion in glassy state polymer films. Phys Rev Lett 2002;89.

223. Schuster R, Barth M, Gruber A, Cichos F. Defocused wide field fluorescence imaging of single CdSe/ZnS quantum dots. Chem Phys Lett 2005;413:280–283.

224. Hellen EH, Axelrod D. Fluorescence emission at dielectric and metal-film interfaces. J Opt Soc Am B 1987;4:337–350.

225. Richards B, Wolf E. Electromagnetic diffraction in optical systems. II. Structure of the image field in an aplanatic system. Proc R Soc Lond A Math Phys Sci 1959;253:358–379.

226. Klimov VV, Ducloy M. Quadrupole transitions near an interface: general theory and application to an atom inside a planar cavity. Phys Rev A 2005;72.

227. Tang Y, Cook TA, Cohen AE. Limits on fluorescence detected circular dichroism of single helicene molecules. J Phys Chem A 2009.